[Article ID] 1003 - 6326(2000)04 - 0456 - 04

Morphology and growth mechanism of borides in Ti-48Al + B alloys①

LI Zhen-xi(李臻熙), CAO Chun-xiao(曹春晓)
(Beijing Institute of Aeronautical Materials, Beijing 100095, P.R.China)

[Abstract] The morphology and growth mechanism of borides in Ti-48Al + (0.2% ~ 0.8%)B (mole fraction) alloys were investigated. The results show that TiB_2 phase are all flakes with width < 0.5 μm and aspect ratio > 100 in alloys containing 0.2% and 0.5%B, respectively, but there are a few hexagonal blocky borides with habit planes of (0001) and $\{10\bar{1}0\}$ type besides flakes in the alloy containing 0.8%B. Flake borides are the products of irregular eutectic reactions growing coupled with matrix and blocky borides are primary TiB_2 phases growing unconstrained in melt.

[Key words] TiAl alloy; boride; morphology; growth mechanism
[CLC number] TG146 [Document code] A

1 INTRODUCTION

Titanium aluminides have attracted significant interest for high-temperature application due to their good elevated-temperature mechanical properties, high creep and oxidation resistance, low density as well as high modulus[1~3]. Boron additions (< 0.8%) are shown to be effective in refining the grain size and preventing grains from growing rapidly during heat treatment[3]. Smaller additions of boron are shown to refine and stabilize the lamellar structure, therefore, improve mechanical properties[4~6]. It is important to understand the effects of morphology and distribution of the borides on microstructure modification. In this article, the morphology and growth mechanism of the borides in Ti-48Al + (0.2% ~ 0.8%) B casting alloys are investigated.

2 EXPERIMENTAL

The raw materials were 0-grade sponge titanium, high purity aluminum (99.99%) and Al-Ti-B intermediate alloy. Alloys of nominal composition Ti-48Al-0.2B(4802), Ti-48Al-0.5B(4805) and Ti-48Al-0.8B(4808) (mole fraction, %) were prepared by vacuum nonconsumable electrode arc melting. Morphologies of the borides were observed by optical and transmission electron microscopy (JEM-200CX). TEM foils were prepared in a twin jet electropolish unit using a solution of 59% methanol, 35% butyl cellusolve and 6% perchloric acid and operating at -30 ℃ and 40 V. Optical and TEM specimens were as-cast materials.

3 RESULTS

The optical images of as-cast microstructure of three alloys with different B additions are shown in Fig.1. The matrix is $\alpha_2 + \gamma$ lamellar microstructure. The long and thin flakes that distribute at both grain boundaries and interiorities are borides. As shown in Figs.1(a) ~ (c), the white microstructures at grain boundaries and boride/matrix interfaces are equiaxed γ grains formed due to interdendritic segregation. The borides shown in Figs.1(a) ~ (c) are all curved flakes with high aspect ratio and some are branched. Except for the flaky borides, other morphologies of borides can not be found in Fig.1. In a lower magnification image (Fig.1(d)), the boride distribution in the 4808 alloy shows a dendritic feature.

TEM results show that the borides are all flakes in the 4802 and 4805 alloys, but a few blocky borides besides flaky borides are found in the 4808 alloy. It is verified that the two types of boride are both TiB_2 phase with C32 structure by the selecting area diffraction patterns. The typical TEM images and diffraction patterns of the flaky and blocky borides in the 4808 alloy are shown in Fig.2 and Fig.3, respectively. The width of the flaky boride is about 0.3 μm and the aspect ratio is more than 100. The blocky boride shows a hexagonal morphology, its surfacial and peripheral planes are confirmed to be (0001) basal plane and $\{10\bar{1}0\}$ prismatic planes (marked in Fig.3), by the analysis of the diffraction pattern of [0001] zone axis. The ledges on the $\{10\bar{1}0\}$ prismatic planes (marked by arrows) suggest that growth of the blocky TiB_2 phase is expected to take place by a ledge mechanism. The size (< 1 μm) of the blocky boride is too small to be identified in the optical micrographs (Fig.1). Without any orientation relationship is found among the flaky, blocky TiB_2 phase with the γ and α_2 matrix phases.

4 DISCUSSION

The solubility of boron in the γ and α_2 matrix

① [Received date] 1999-07-30; [Accepted date] 1999-10-20

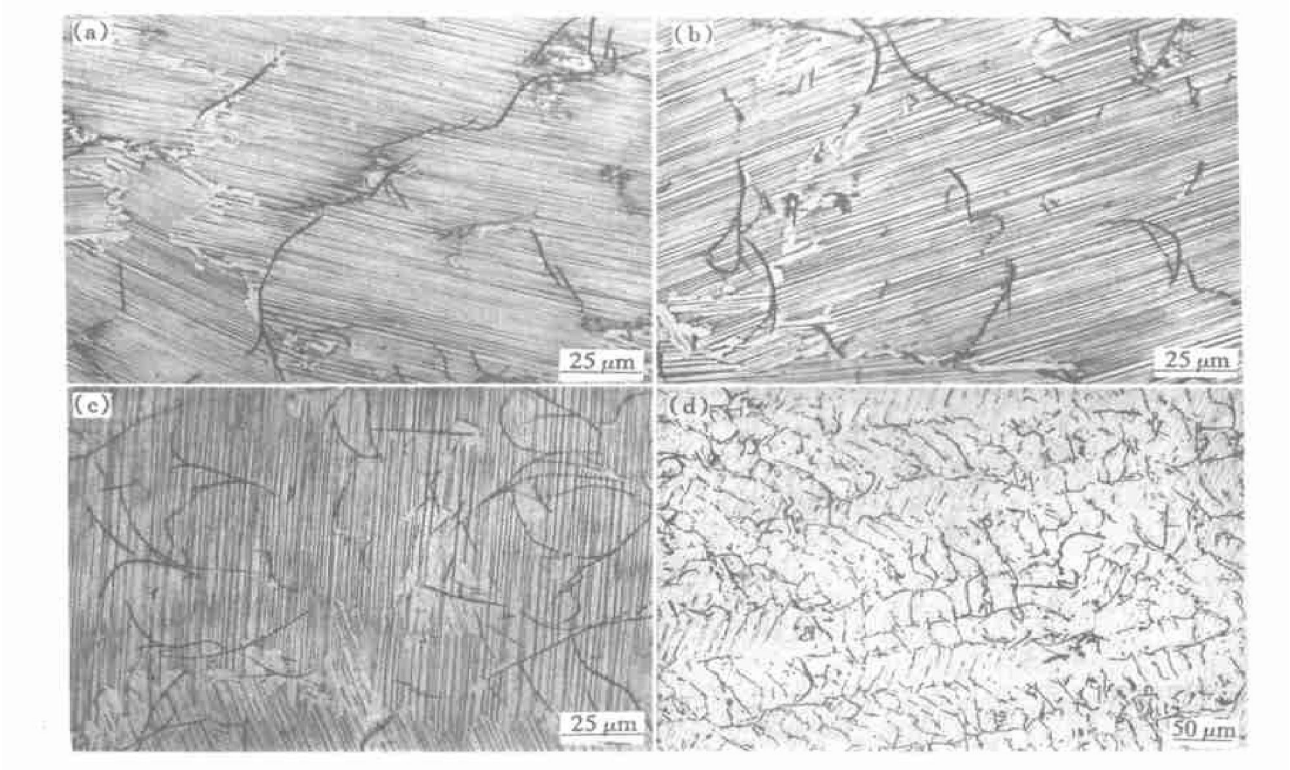

Fig .1 Optical images of borides

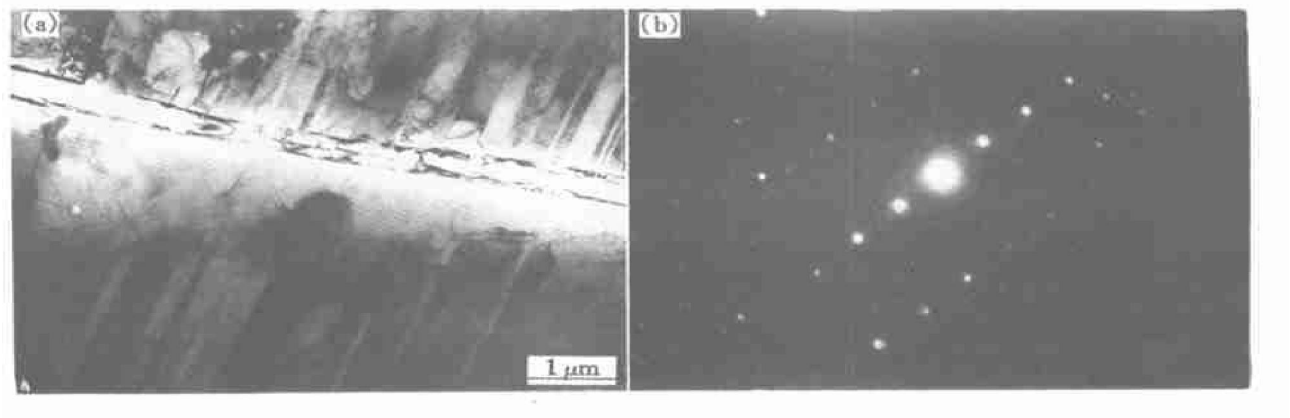

Fig .2 TEM image and SAD pattern ($B=[\bar{2}\bar{1}\,\bar{1}\,6]$) of flaky TiB_2

(a) —TEM image ; (b) —SAD pattern ($B=[\bar{2}\bar{1}\,\bar{1}\,6]$)

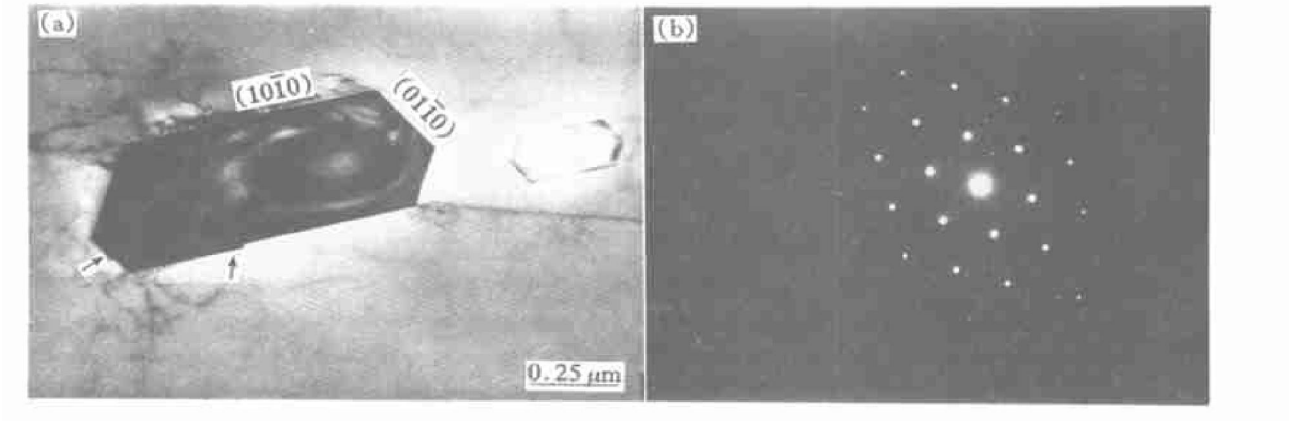

Fig .3 TEM image and SAD pattern ($B=[0001]$) of blocky TiB_2

(a) —TEM image ; (b) —SAD pattern ($B=[0001]$)

phases is found to be only about 0.011 % and 0.003 %, respectively[7]. The majority of boron in TiAl alloys is contained in the refractory TiB_2 phases. The crystal structure of TiB_2 is C32 type (a = 0.303 nm, c = 0.323 nm) which consists of close-packed Ti-atom planes (A) stacked with graphite-like B-atom planes (H) in a AHAH …sequence along the c-axis of the crystal, as shown in Fig.4.

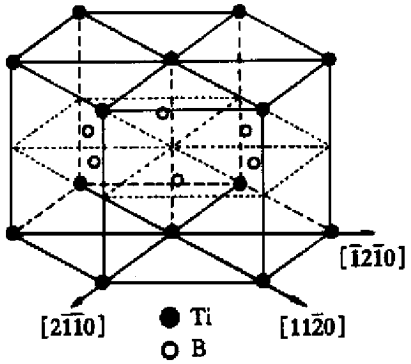

Fig.4 Crystal structure of TiB_2 (C32 type)

Fig.5 shows part of liquidus projection for Ti-Al-B system in the vicinity of equiatomic TiAl composition[8], the positions of three alloys used in this article are marked in the phase diagram. The primary phases of three alloys are all β phases, the solidified β phase then transforms to $\alpha_2 + \gamma$ phases by the following sequence of solid-state transformation:

$$\beta \rightarrow \alpha \rightarrow \alpha + \gamma \rightarrow \alpha_2 + \gamma$$

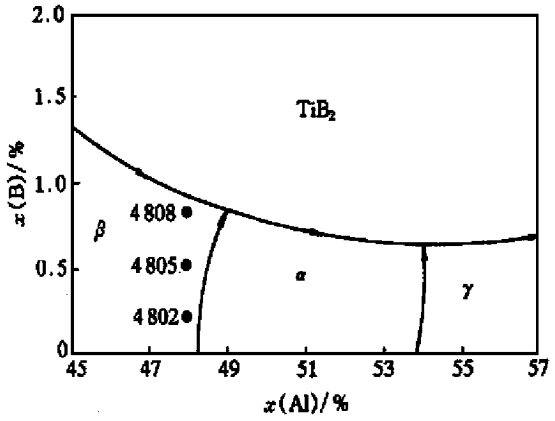

Fig.5 Part of liquidus projection for Ti-Al-B system[8]

The composition of 4808 alloy is so close to the monovariant line of $L \rightarrow \beta + TiB_2$ reaction that the B contents of some areas in the melt would be higher than the monovariant line due to composition undulation in the melt. Therefore, a few primary TiB_2 nuclei would form in these B concentrated areas. While, the majority of borides is the secondary TiB_2 which would nucleate and grow concurrently with the matrix by the reactions of $L \rightarrow \beta + TiB_2$ and $L + \beta \rightarrow \alpha + TiB_2$. Hyman, et al[8,9] have demonstrated that blocky boride is primary TiB_2 that nucleates and grows unconstrained in melts and flaky boride is the secondary TiB_2 that nucleates after primary matrix phase and grows coupled with matrix. Consistent with the results of Ref.[8], the habit planes of the blocky TiB_2 in the 4808 alloy are (0001) basal plane and prismatic $\{10\bar{1}0\}$ planes, as shown in Fig.3, however, the blocky TiB_2 size (< 1 μm) in the 4808 alloy is significantly smaller than that in Ti-50.4Al-1.33B alloy (10 ~ 20 μm)[8]. Since the major primary phase solidified in the melt of 4808 alloy is β phase, a few primary TiB_2 nuclei would be trapped and constrained rapidly by β grains after they formed. Thus, the TiB_2 nuclei can not grow into large size borides. On the other hand, the primary TiB_2 can not directly form in the melts of 4805 and 4802 alloys because of the lower B contents. The borides would form by the eutectic reactions until the liquid compositions reach the $L \rightarrow M + TiB_2$ (M = α, β and γ) monovariant line after the matrix phases formed in the melts. Therefore, only the secondary flaky TiB_2 growing concurrently with the matrix are found in 4805 and 4802 alloys.

As shown in Fig.3, growth of the blocky TiB_2 is expected to take place by a ledge mechanism. Because primary TiB_2 nucleates and grows freely in melt before matrix phases form, the morphology would be determined by the slowest growing facets in the crystal. The sequence of the bond strength in TiB_2 crystal is B-B > Ti-B > Ti-Ti[10]. Calculations of the attachment energy for various low-index crystal planes of the TiB_2 phase suggest the following hierarchy of growth rates[10]:

$$(0001) < \{10\bar{1}0\} < \{10\bar{1}1\} < \{1\bar{2}10\} < \{1\bar{2}11\}$$

The ranking essentially reflects the density of strong bonds in the various crystal planes. The stacking sequence on the (0001) basal plane and prismatic $\{10\bar{1}0\}$ planes is a plane containing all Ti atoms stacked alternatively with a plane containing all B atoms as shown in Fig.4. Thus, the growth rates normal to these planes are the lowest. The analysis is consistent with the experimental results shown in Fig.3 that the habit planes of the primary TiB_2 are the (0001) and $\{10\bar{1}0\}$ crystal planes. However, morphology of the secondary TiB_2 would be affected by diffusional effects and physical constraints imposed by matrix, because it grows coupled with the matrix by the eutectic reactions. The habit plane of secondary TiB_2 is $\{1\bar{2}10\}$ type[8]. It is different from the primary TiB_2 because of the need for faster propagation rates to sustain coupled with growth with the matrix. The convoluted flaky morphology demonstrates that the secondary TiB_2 is a product of irregular eutectic reaction.

5 CONCLUSIONS

1) Only the flaky borides with width $< 0.5\ \mu m$ and aspect ratio > 100 are found in the 4802 as well as 4805 alloys, but there are two types of borides with different morphologies, flaky and hexagonal blocky, in the 4808 alloy. The size of blocky boride is less than 1 μm. It is verified that the two types of borides both are TiB_2 phase with C32 structure.

2) The hexagonal blocky borides with habit planes of (0001) and $\{10\bar{1}0\}$ types are primary TiB_2 phases that nucleate and grow in melt. The flaky borides are secondary TiB_2 growing coupled with the matrix by the eutectic reactions of $L \rightarrow \beta + TiB_2$ and $L + \beta \rightarrow \alpha + TiB_2$.

[REFERENCES]

[1] Kim Y W. Effects of microstructure on the deformation and fracture of γ-TiAl alloys [J]. Mater Sci Eng, 1995, 192/193A: 519.

[2] PENG Cao-qun, HUANG Bai-yun and HE Yue-hui. Effect of alloying on properties of TiAl-based alloys and mechanisms [J]. The Chinese Journal of Nonferrous Metals, 1998, 8(Suppl.1): 12.

[3] Kim Y W and Dimiduk M. Designing gamma TiAl alloys. Fundamental, Strategy and Production [A]. Nathal M V et al. Structure Intermetallics 1997. TMS [C]. Warrandale, 1997. 531.

[4] Graef M D, Hardwick D A and Martin P L. Structure evolution of titanium diborides in wrought Ti-47% Al-2% Mo-0.2% B [A]. Nathal M V. Structure Intermetallics 1997. TMS [C]. Warrandale, 1997. 185.

[5] Krishnan M, Nalarajan B, Vasudevan V K, et al. Microstructure evolution in gamma titanium aluminides containing beta-phase stabilizers and boron additions [A]. Nathal M V. Structure Intermetallics 1997. TMS [C]. Warrandale, 1997. 235.

[6] Ramanjan R V, Maziasz P J and Liu C T. The thermal stability of the microstructure of γ-based titanium aluminides [J]. Acta Mater, 1996, 44(7): 2611.

[7] Larson D J, Liu C T and Miller M K. Microstructural characterization of segregation and precipitation in $\alpha_2 + \gamma$ titanium aluminides [J]. Mater Sci Eng, 1997, A239/240: 220.

[8] Hyman M E, Mccullough C, Valencia J J, et al. Evolution of boride morphologies in TiAl-B alloys [J]. Metall Trans, 1991, 22A(7): 1647.

[9] Hyman M E, Mccullough C, Levi C G, et al. Microstructure evolution in TiAl alloys with B additions: conventional solidification [J]. Metall Trans, 1989, 20A(9): 1847.

[10] Abel-Harvid A A, Hamar-Thibault S and Hamar R. Crystal morphology of the compound TiB_2 [J]. J Cryst Growth, 1985, 71: 744.

(Edited by YANG Bing)